Color Perception: Controlled Excitation of Opponent Channels

Prashanth Alluvada
Electrical and Computer Engineering
Jimma University
Ethiopia
Email: prashanthalluvada@gmail.com

Abstract

We describe controlled excitation of opponent color channels. For monochromatic impingement of spectral energy, the wavelength sequences we develop cause a channel to attain a preset excitation level, causing thereby a controlled excitation of color channels.

1. Introduction

Spectral energy captured by the cones is encoded through two opposing channels. The viewpoint we adopt here is that a certain degree of control may be imparted into color encoding mechanism through controlled impingement of spectral energy. For this purpose, in this article, we use monochromatic type spectral energy impingement.

2. Controlled Excitation of Color Channels

Opponent Color Theory asserts that opponent channels are encoded according to

$$F_1 = X - Y \tag{1a}$$
$$F_2 = Z - X - Y \tag{1b}$$

where the X, Y and Z are the tri-stimulus values from the XYZ color theory. Here, the F1 and F2 are referred as excitation levels of the channels. Eqns. ((1a),(1b)) imply that their linear combination, shown at Eqn. (2), must vanish:

$$F_1 (Z - X - Y) - F_2 (X - Y) = 0 \tag{2}$$

When the impinging energy is monochromatic then the X, Y and Z are given by

$$\begin{aligned} X &= h\,\mathrm{x}(\lambda) \\ Y &= h\,\mathrm{y}(\lambda) \\ Z &= h\,\mathrm{z}(\lambda) \end{aligned} \tag{3a-c}$$

where the "h" refers to the intensity of the monochromatic energy at wavelength λ.

This is the "spike type" of spectral radiance distribution. Using Eqn.(3) in Eqn.(2) we get the following linear combination:

$$F_1\, h\,(z(\lambda) - x(\lambda) - y(\lambda)) - F_2\, h\,(x(\lambda) - y(\lambda)) = 0 \qquad (4)$$

which implies that Eqn. (4) is independent of the h. We let the F1 and F2 be constants C1 and C2 respectively and generate solutions of Eqn. (4). With this notation Eqn. (4) takes the forms (Eqns. (5a), (5b))

$$C_1\,(z(\lambda) - x(\lambda) - y(\lambda)) - C_2\,(x(\lambda) - y(\lambda)) = 0 \qquad (5a)$$

$$C_1\,(z(\lambda) - x(\lambda) - y(\lambda)) = C_2\,(x(\lambda) - y(\lambda)) \qquad (5b)$$

Define the functions G1 and G2 from Eqn. (5), in the following fashion:

$$G_1(\lambda) = z(\lambda) - x(\lambda) - y(\lambda)$$
$$G_2(\lambda) = x(\lambda) - y(\lambda) \qquad (6a\text{-}b)$$

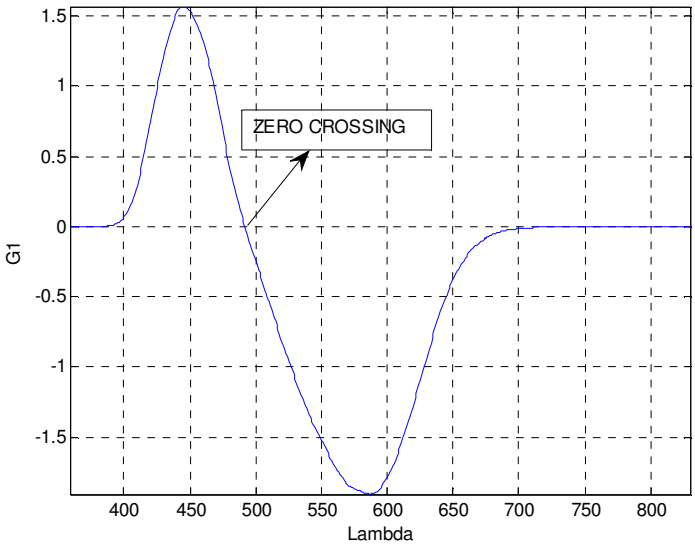

Fig. 1. A plot of G1 (Eqn. (6a)).

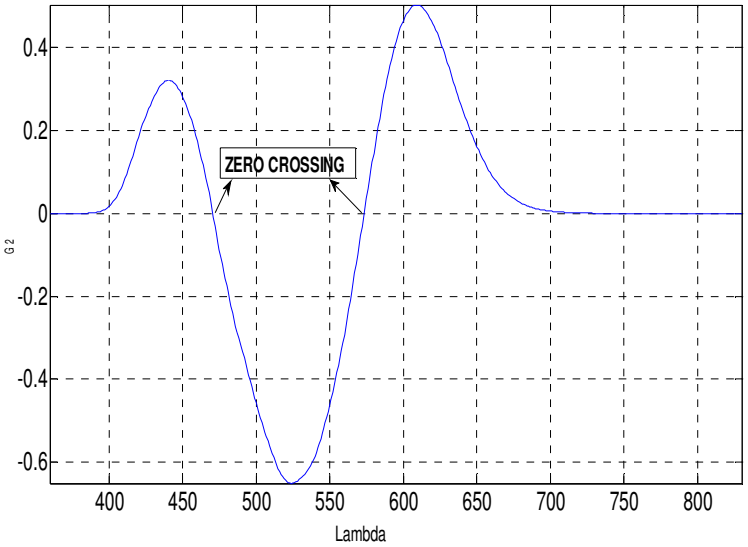

Fig. 2. A plot of G2 (Eqn. (6b)).

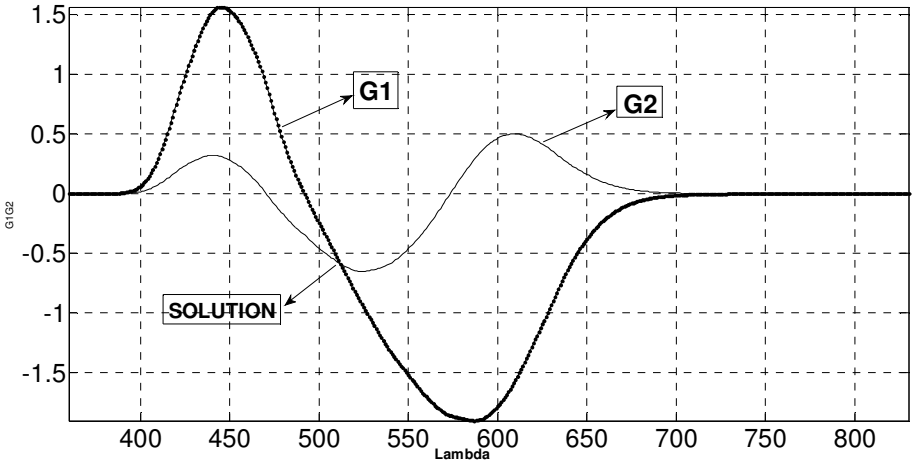

Fig. 3a. A solution point is obtained as the intersection of G1 and G2 curves. In this case, C1=1 and C2=1. See Eqn. (5b).

The constants C1, C2 together with the functions G1, G2 determine the solutions of Eqn. (5). Eqn. (5) is solved in the following fashion. For a given C1 and C2, both constant, we seek the set of all wavelengths lambda so that Eqn. (5a), (equivalently Eqn. (5b)) is true. They are the roots of Eqn. (5a). An instance of this solving method is depicted in Figs. ((3a), (3b), (3c)) Ordinate at the point marked "solution" (Fig. (3b)) is the intensity of the spike type spectral radiance distribution, h. In this situation the h is negative. To compute the h from C1 and C2, we use Eqns. ((1), (6)), through the following equations

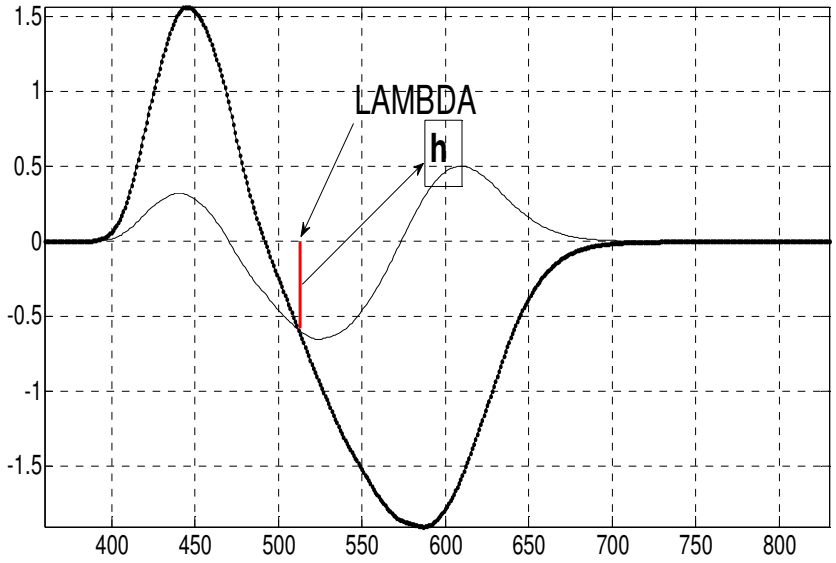

Fig. 3b. The h and lambda are read off from the solution. As in Fig. (3a), the ordinate at the intersection "solution" point is the height h of the spike type monochromatic spectral radiance. The h is the red vertical line here.

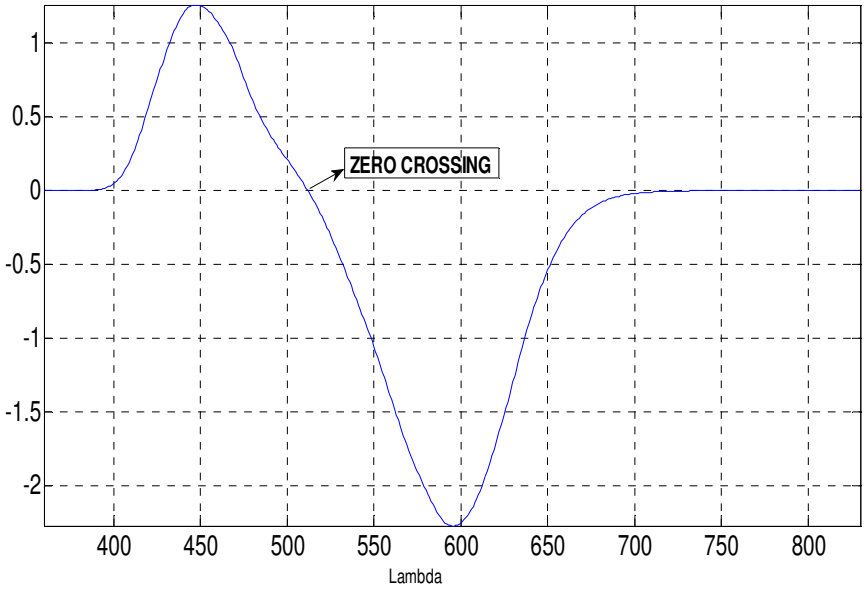

Fig. 3c. This is Eqn. (5a), C1 and C2 are both unity.

$$h_1 = \frac{F_1}{G_2}$$

$$h_2 = \frac{F_2}{G_1} \qquad (7a, b)$$

The h1 and h2 are nearly equal, the h is computed as an average of h1 and h2.

$$h = \frac{1}{2}h_1 + \frac{1}{2}h_2 \tag{8}$$

Now when the C1 is kept constant and the C2 is varied, then we have a sequence of (h,lambda) for varying C2, which render F1=C1, a constant. Therefore we have monochromatic energy sequences (h,lambda) that render the excitation level of the first channel, F1, invariant. So that these energy sequences fix the excitation level of the first opponent channel F1 to a constant C1. We are showing some solutions of Eqn. (5) in Table 1 (Appendix).

3. Instances of multiple roots

Eqn. (5) can admit multiple solution for a given C1 and C2. For example, for each pair C1 and C2 shown at Table 2, Eqn. (5) admits a pair of roots, tabulated there. Following symmetry is clear: if the pair (C1,C2) admits a pair of roots then so does the pair (-C1,-C2). C1 and C2 are the channel excitations. Three roots were also found to occur.

TABLE 2

S. No.	C1	C2	LAMBDA1	LAMBDA2
(a)	-1.3750	8.0010	476.083	589.135
(b)	-2.0625	-12.0001	452.943	559.975
(c)	0.6875	-12.0001	472.778	578.241
(d)	0.6875	8.0010	465.212	566.546

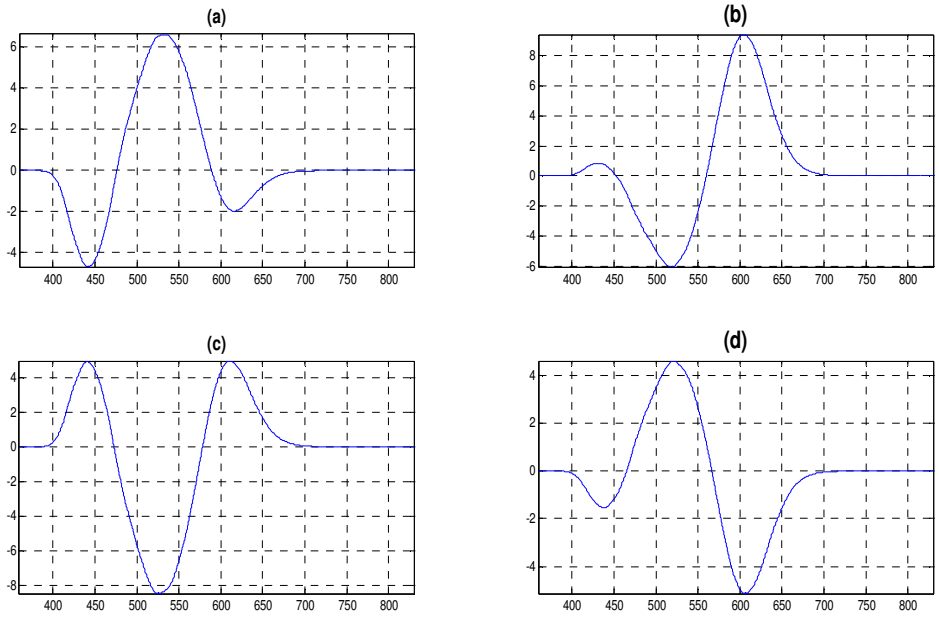

Fig. 4. For the C1 and C2 combinations displayed at Table 2, Eqn. (5) admits a pair of roots shown in these four graphs (a), (b), (c), (d).

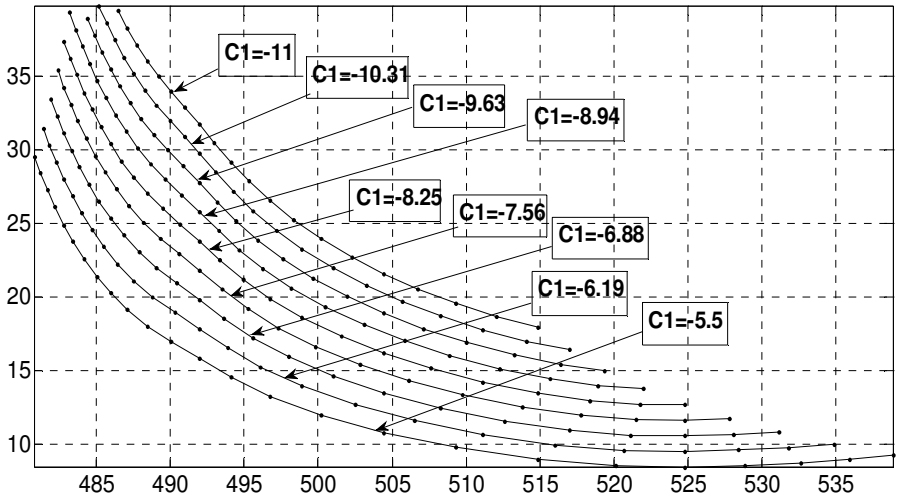

Fig. 5. Spike sequences corresponding to constant C1. C2 is variable. Abscissa has wavelength

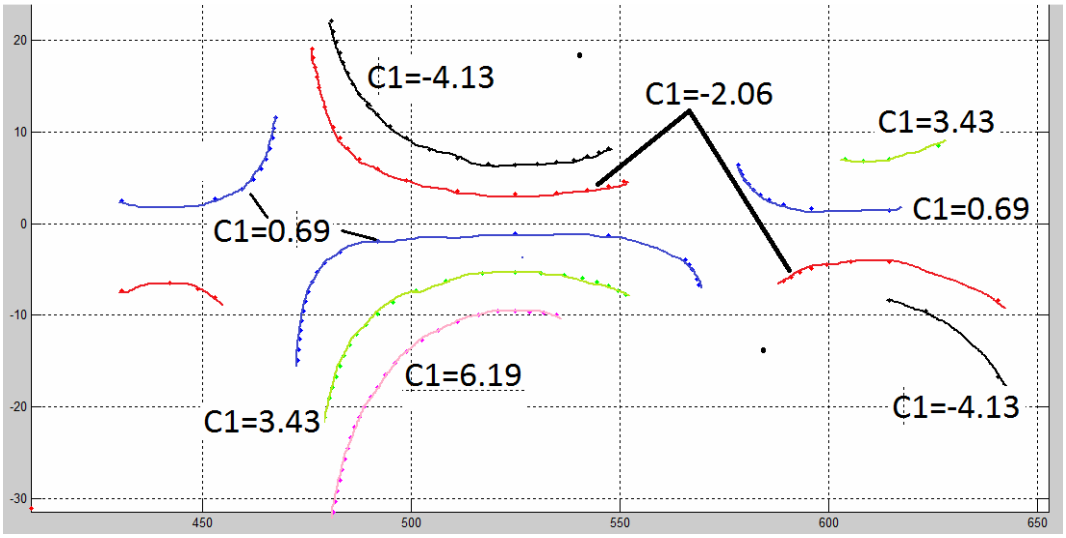

Fig. 6. Spike sequences corresponding to constant C1. For these C1, the sequences occur as disconnected subsets, here marked using a color code. For example: for C1=0.69, the spike sequences occur as three disconnected sets marked in blue. C2 could be variable along these curves. Abscissa has wavelength. Table 3 shows the C1 values and the color code used.

Table 3		
S. No.	Color	C1
1	BLACK	-4.13
2	RED	-2.06
3	BLUE	0.69
4	GREEN	3.43
5	MAGENTA	6.19

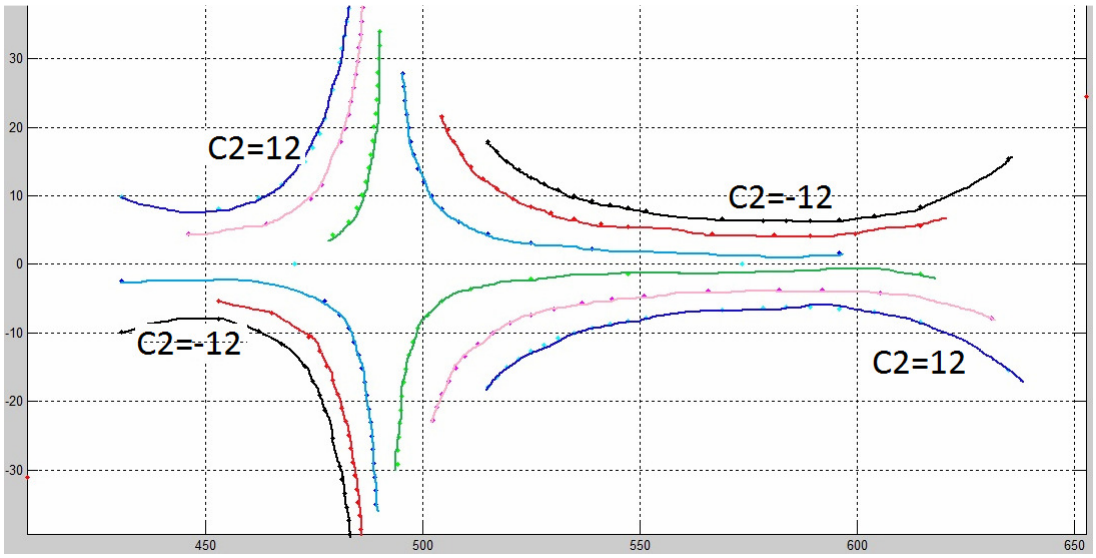

Fig. 7. Spike (h) sequences corresponding to constant C2. Color code and C2 values are at Table 4. C1 is variable along these curves.

Table 4		
S. No.	Color	C2
1	BLACK	-12
2	RED	-8
3	CYAN	-3
4	GREEN	2
5	MAGENTA	7
6	BLUE	12

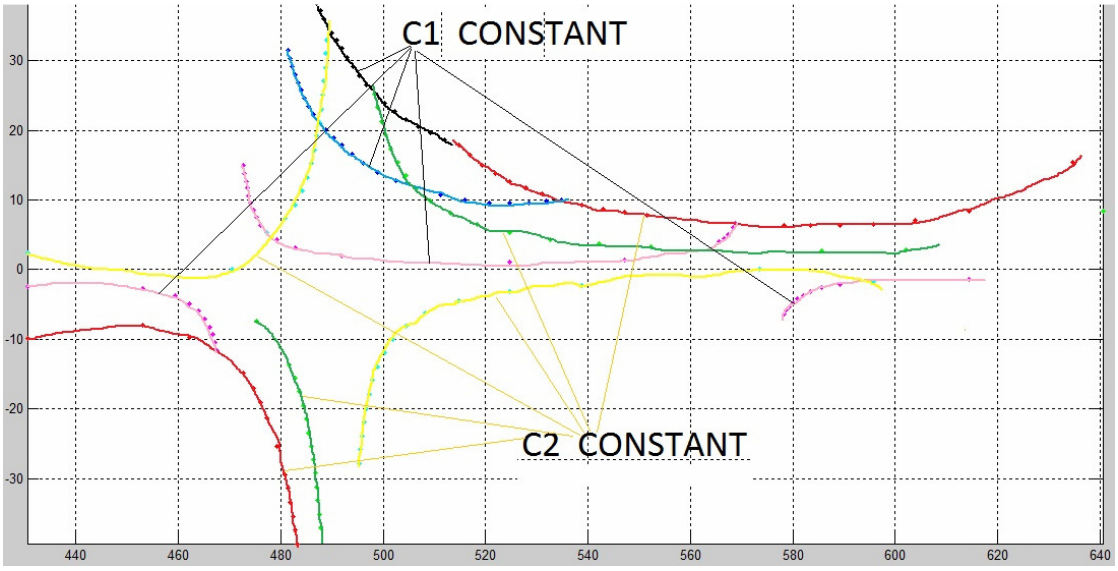

Fig. 8. C1 constant and C2 constant curves in same plot. Table 5 has the data and the color code used. This plot shows that C1 constant data is distinct from C2 constant data.

TABLE 5: C1 Const and C2 Const in same plot				
	C1	C1 COLOR	C2	C2 COLOR
1	-11.00	BLACK	-12	RED
2	-6.18	BLUE	-5	GREEN
3	-0.69	MAGENTA	3	YELLOW

TABLE 6								
S. No.	LAMBDA	h	X	Y	Z	x	y	z
1	534.8575	9.9748	3.0148	9.2016	0.2077	0.2427	0.7406	0.0167
2	531.8022	9.7735	2.5446	8.7314	0.2572	0.2206	0.7571	0.0223
3	528.4178	9.6198	2.0777	8.2643	0.3307	0.1947	0.7743	0.0310
4	524.7985	9.5106	1.6224	7.8084	0.4152	0.1648	0.7930	0.0422
5	520.6621	9.5715	1.1914	7.3761	0.5543	0.1306	0.8086	0.0608
6	516.0086	9.9524	0.7983	6.9824	0.7744	0.0933	0.8162	0.0905
7	511.1201	10.6615	0.4690	6.6544	1.1119	0.0569	0.8080	0.1350
8	506.5137	11.6162	0.2480	6.4346	1.6684	0.0297	0.7705	0.1998
9	502.5183	12.6950	0.1052	6.2916	2.3809	0.0120	0.7168	0.2712
10	498.8989	13.9606	0.0436	6.2304	3.2662	0.0046	0.6531	0.3424
11	496.0786	15.2550	0.0627	6.2471	4.3036	0.0059	0.5886	0.4055
12	493.8694	16.5478	0.1147	6.3029	5.3870	0.0097	0.5339	0.4564
13	491.9422	17.8425	0.1948	6.3835	6.5627	0.0148	0.4858	0.4994
14	490.2970	18.9628	0.2944	6.4865	7.7450	0.0203	0.4465	0.5332
15	488.7929	20.0050	0.4119	6.5951	8.9742	0.0258	0.4127	0.5615
16	487.5238	21.1006	0.5579	6.7378	10.2675	0.0318	0.3836	0.5846
17	486.4426	22.2346	0.7179	6.8970	11.5890	0.0374	0.3591	0.6035
18	485.5026	23.4059	0.8893	7.0697	12.9443	0.0425	0.3382	0.6192
19	484.7035	24.5615	1.0620	7.2455	14.2763	0.0470	0.3208	0.6321
20	483.9984	25.7222	1.2380	7.4255	15.6111	0.0510	0.3059	0.6431
21	483.3873	26.8496	1.4202	7.6028	16.9450	0.0547	0.2928	0.6525
22	482.8233	28.0022	1.6000	7.7867	18.2810	0.0578	0.2814	0.6607
23	482.3062	29.1629	1.7895	7.9755	19.6628	0.0608	0.2710	0.6682
24	481.8362	30.3121	1.9729	8.1614	21.0090	0.0633	0.2621	0.6746
25	481.4131	31.4274	2.1571	8.3483	22.3544	0.0656	0.2541	0.6803

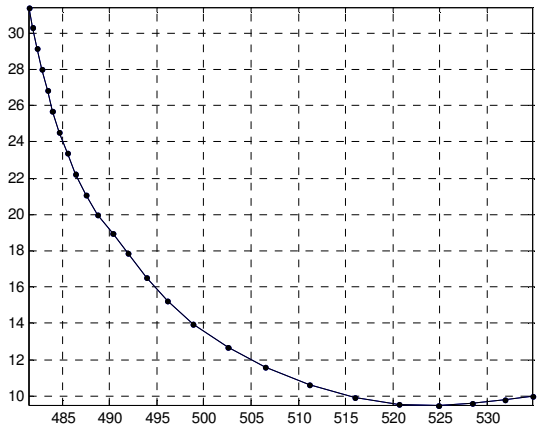

Fig. 9. This is spike sequence from Fig. 5 corresponding to C1=-6.19. We show further calculation for this spike sequence.

Computing the tri-stimulus values of this sequence of spikes, h (Fig. 9).

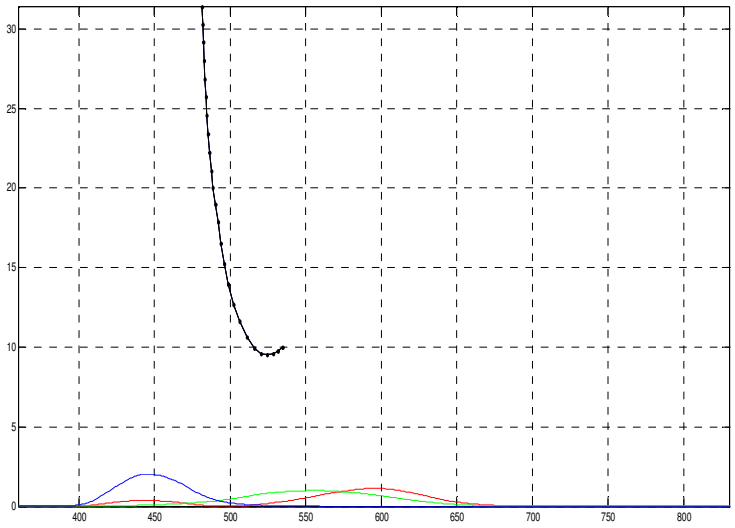

Fig. 10. The sequence of spikes (h, lambda), marked black, are overlaid with the color matching functions of XYZ color space.

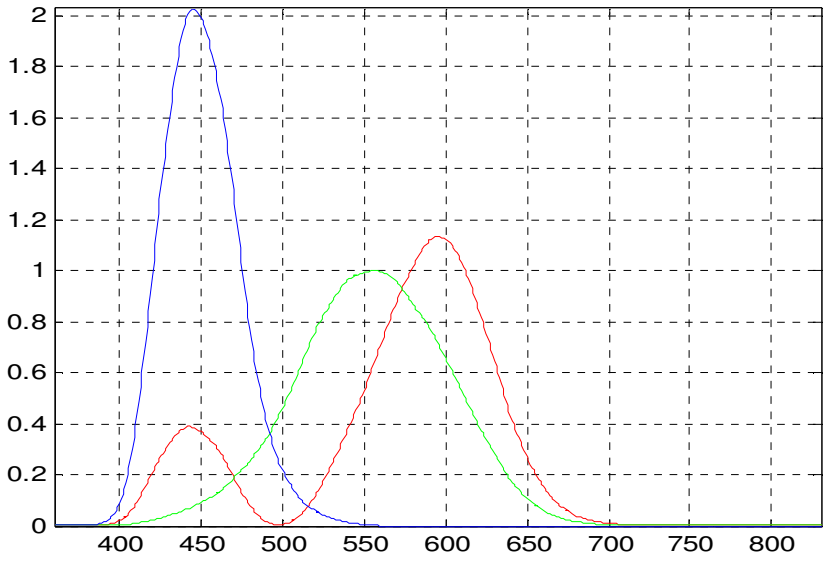

Fig. 11. The color matching functions of XYZ color space.

4. Comparing Spike Sequences

Spike sequences corresponding to constant C1 and constant C2 are shown plotted in Figs. (5-8) for relative comparison. Further calculation is made for C1=-6.19 from Fig. 5, shown at Fig. 9.

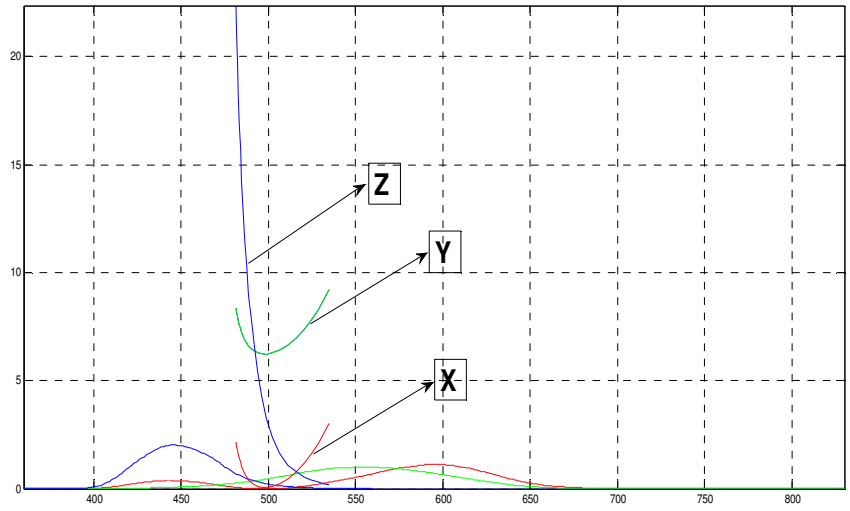

Fig. 12. The tri-stimulus values X, Y, Z corresponding to the sequence of h-spikes at Table 6. The h-spikes curve is shown overlaid with the XYZ color matching functions at Fig. 10, marked black.

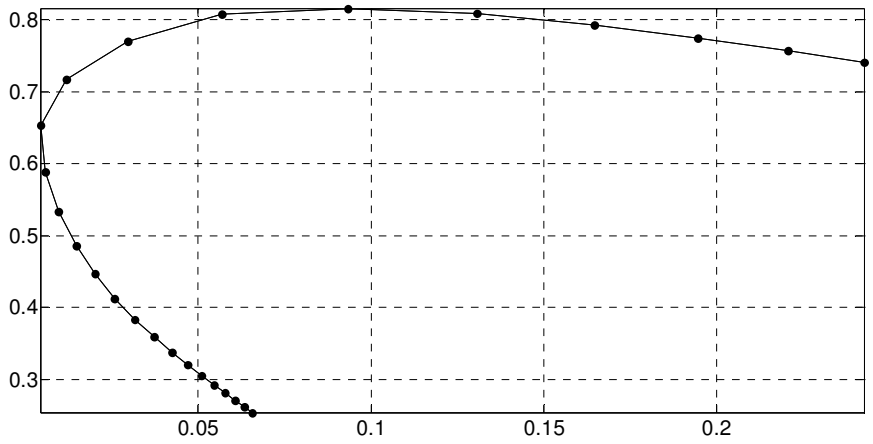

Fig. 13. The plot of (x,y) from XYZ color space corresponding to the (h, lambda) of Table 6. The (x,y) are tabulated at Table 6. This is a subset of the spectral locus.

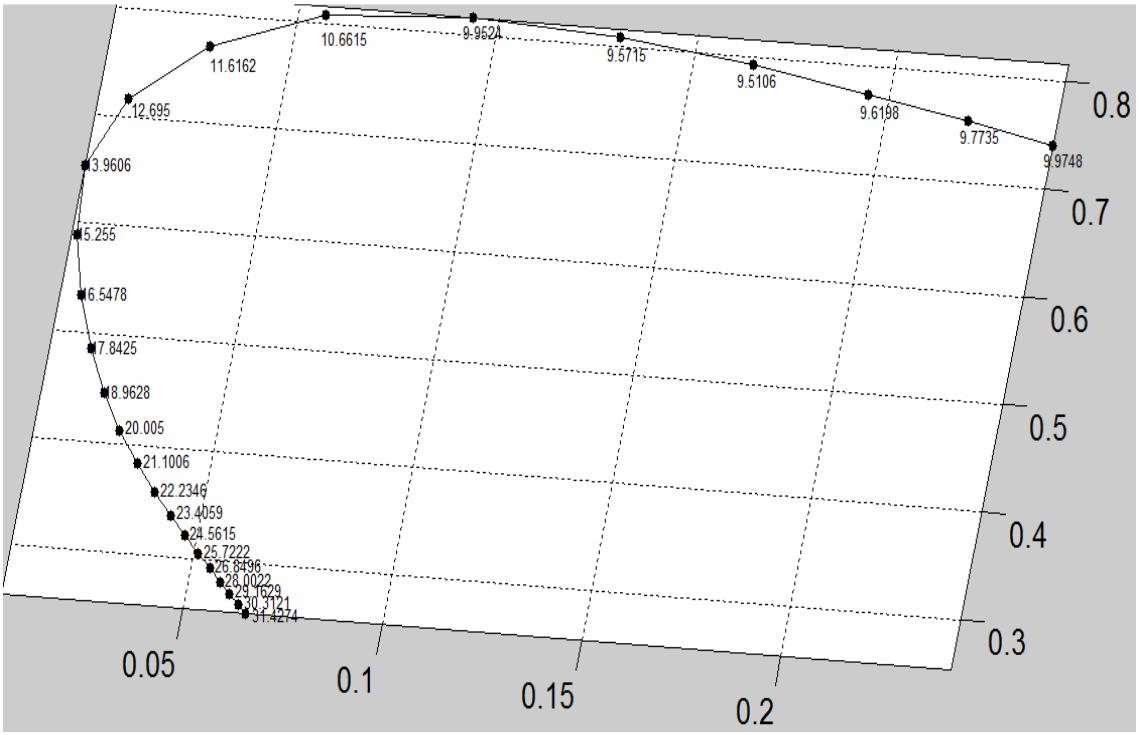

Fig. 14. The spike heights are marked along the curve. The curve is a subset of the spectral locus. The data is at Table 6.

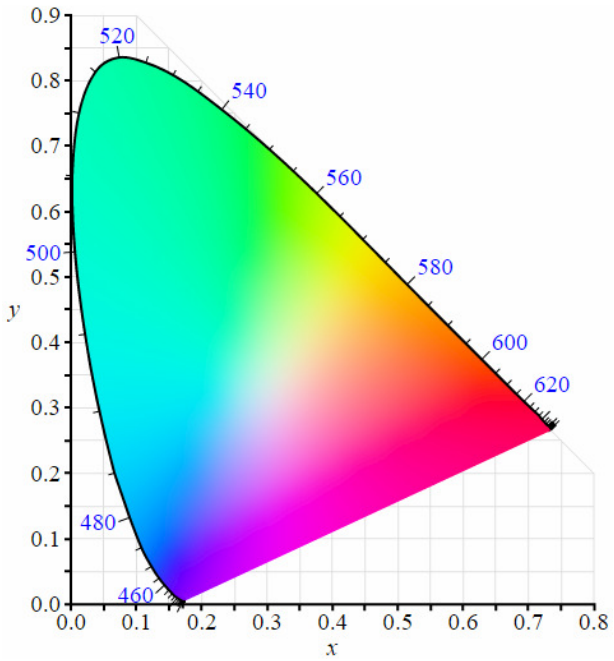

Fig. 15. The 1931 CIE chromaticity diagram in (x,y) coordinates based on XYZ system. This is for locating the data at Fig. 14 along the spectral locus.

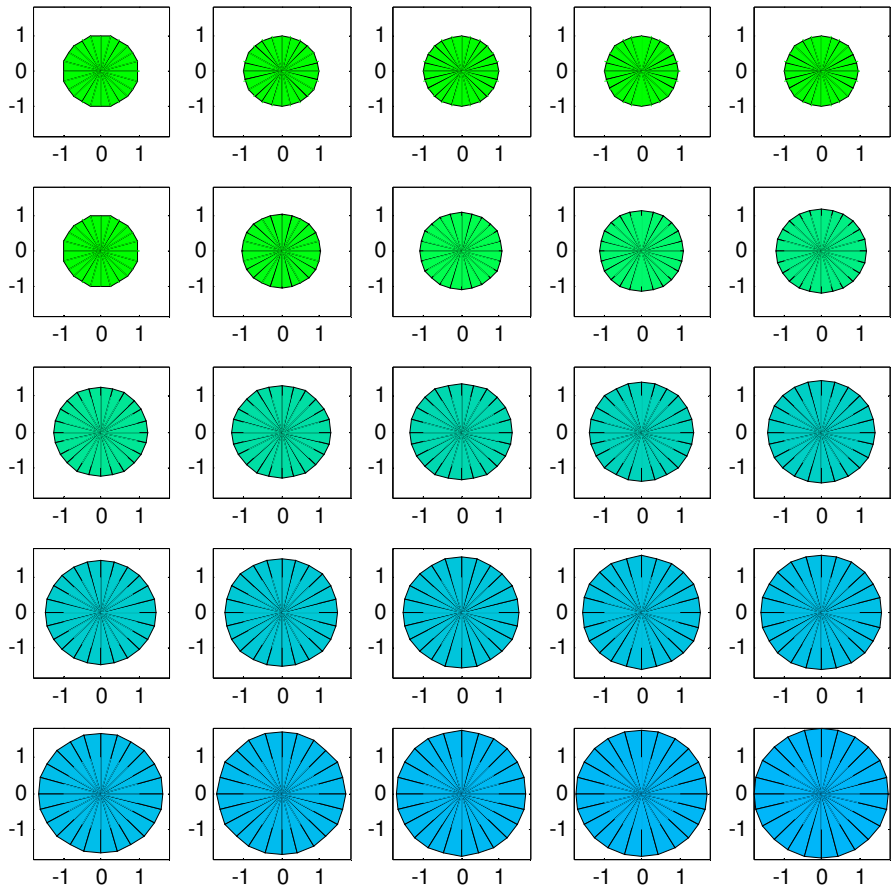

Fig. 16. The color disks show the color sequence yielded by the spike (h) sequence at Table 6. The sequence goes left to right at each row. The area of the disk is proportional to the energy (height) of the spike, so that such disks of varying area impinging a designed color sequence can cause a channel excitation to be a constant.

5. Conclusion and Future Work

We described a method of exciting the opponent channels in a controlled manner. This knowledge would help design color perception experiments and related psychophysical experiments through which a better understanding of human color perception's information encoding mechanism is possible. This understanding should lead to new hypotheses about internal encodings among the sensory and motor pathways of other systems. In future articles we'll describe further methods which can impart new types of control upon the internal encoding channels of human color perception.

References

1) Kaiser, PK and Boynton, RM (1996), "Human Color Vision," Optical Society of America, Second edition.
2) "Opponent Process," https://en.wikipedia.org/wiki/Opponent_process
3) Prashanth, A., (2016), "Color Perception: Controlled Excitation of Opponent Channels," Global Journal for Research Analysis, Vol. 5, Issue 9, September 2016. (https://www.worldwidejournals.com/global-journal-for-research-analysis-GJRA/file.php?val=September_2016_1474362810__132.pdf)
4) Prashanth, A., (2016), "A Cost Function for Complex Systems," International Journal of Scientific Research, Vol. 5, Issue 12, December 2016. (https://www.worldwidejournals.com/international-journal-of-scientific-research-(IJSR)/recent_issues_pdf/2016/December/December_2016_1480597760__204.pdf)
5) arxiv: 'submit/1639428': "Color Perception: Controlled Excitation of Opponent Channels," submitted August 15, 2016. (https://arxiv.org)
6) arxiv: 'submit/1441090': "A Cost Function for Complex Systems," submitted December 27, 2015. (https://arxiv.org)

APPENDIX

TABLE 1

S. No.	C1	C2	LAMBDA	h1	h2	h=(h1+h2)/2
1	-11	-12	514.83	17.944	17.912	17.928
2	-11	-2	494.1	29.154	28.669	28.912
3	-11	8	485.97	40.527	41.003	40.765
4	-10.313	-7	503.27	20.784	20.733	20.758
5	-10.313	3	489.07	32.989	33.708	33.349
6	-9.625	-12	519.35	15.012	14.996	15.004
7	-9.625	-2	494.43	25.192	24.93	25.061
8	-9.625	8	485.41	36.608	37.048	36.828
9	-8.9375	-7	505.86	17.01	16.971	16.991
10	-8.9375	3	488.7	29.002	29.67	29.336
11	-8.25	-12	524.8	12.681	12.658	12.669
12	-8.25	-2	494.9	21.216	21.028	21.122
13	-8.25	8	484.7	32.749	32.969	32.859
14	-7.5625	-7	509.76	13.342	13.326	13.334
15	-7.5625	3	488.18	25.06	25.398	25.229
16	-6.875	-12	531.14	10.822	10.804	10.813
17	-6.875	-2	495.61	17.232	17.057	17.145
18	-6.875	8	483.86	28.858	29.019	28.938
19	-6.1875	-7	516.01	9.9524	9.9438	9.9481
20	-6.1875	3	487.52	21.101	21.382	21.242
21	-5.5	-12	538.85	9.2461	9.2372	9.2416
22	-5.5	-2	496.74	13.261	13.155	13.208
23	-5.5	8	482.82	24.891	25.202	25.047
24	-4.8125	-9	533.59	7.6853	7.676	7.6807
25	-4.8125	1	489.83	14.99	15.307	15.149
26	-4.125	-5	518.36	6.4834	6.4772	6.4803
27	-4.125	5	483.67	17.543	17.658	17.601
28	-3.4375	-12	551.4	7.7951	7.7697	7.7824
29	-3.4375	-2	501.01	7.3229	7.3	7.3114
30	-2.75	-10	552.25	6.4264	6.4068	6.4166
31	-2.75	8	479.34	16.945	17.121	17.033
32	-2.0625	-9	430.55	-7.3597	-7.356	-7.3579
33	-2.0625	1	487.52	7.0335	7.1272	7.0804
34	-2.0625	9	477.37	15.945	16.086	16.015
35	-1.375	-11	563.62	6.3	6.2605	6.2803
36	-1.375	-1	504.45	2.6979	2.692	2.695
37	-1.375	6	595.78	-3.2476	-3.2513	-3.2494
38	-1.375	11	584.49	-5.7647	-5.7935	-5.7791
39	-0.6875	-8	465.24	-7.0507	-7.0228	-7.0367
40	-0.6875	6	474.64	8.4826	8.6178	8.5502
41	-0.6875	11	473	13.807	14.064	13.936
42	0.6875	-9	473.47	-11.675	-11.882	-11.779
43	0.6875	-4	476.15	-6.3534	-6.4555	-6.4044
44	0.6875	4	452.98	2.6834	2.6814	2.6824
45	0.6875	11	568.42	-6.1144	-6.0498	-6.0821
46	1.375	-9	587.22	4.7118	4.73	4.7209
47	1.375	-4	479.34	-8.4727	-8.5607	-8.5167
48	1.375	5	552.25	-3.2132	-3.2034	-3.2083

S. No.	C1	C2	LAMBDA	h1	h2	h=(h1+h2)/2
49	2.0625	-12	476.15	-19.06	-19.367	-19.214
50	2.0625	-6	614.48	4.199	4.2006	4.1998
51	2.0625	3	524.8	-3.1702	-3.1645	-3.1673
52	2.75	-12	477.37	-21.26	-21.448	-21.354
53	2.75	4	524.8	-4.227	-4.2193	-4.2232
54	3.4375	-11	608.18	6.8424	6.8473	6.8448
55	3.4375	-4	483.86	-14.429	-14.51	-14.47
56	3.4375	6	531.14	-5.411	-5.4022	-5.4066
57	4.125	-10	640.48	16.71	16.715	16.712
58	4.125	-1	489.5	-12.997	-13.225	-13.111
59	4.125	9	538.85	-6.9346	-6.9279	-6.9313
60	4.8125	-7	482.82	-21.779	-22.052	-21.916
61	4.8125	3	501.95	-10.011	-9.9917	-10.001
62	5.5	-12	480.8	-29.492	-29.781	-29.636
63	5.5	-4	485.97	-20.264	-20.501	-20.383
64	5.5	6	514.83	-8.972	-8.9558	-8.9639
65	6.1875	-9	482.82	-28.002	-28.353	-28.178
66	6.1875	1	493.87	-16.548	-16.058	-16.303
67	6.1875	11	531.8	-9.7735	-9.7565	-9.765
68	6.875	-4	486.87	-24.184	-24.522	-24.353
69	6.875	6	508.25	-12.471	-12.443	-12.457
70	7.5625	-9	483.76	-31.951	-32.21	-32.081
71	7.5625	1	493.49	-20.522	-19.89	-20.206
72	7.5625	11	524.8	-11.624	-11.603	-11.614
73	8.25	-4	487.52	-28.134	-28.509	-28.322
74	8.25	6	504.45	-16.187	-16.152	-16.169
75	8.9375	-9	484.56	-35.797	-36.278	-36.037
76	8.9375	1	493.26	-24.477	-23.379	-23.928
77	8.9375	11	518.92	-13.984	-13.957	-13.971
78	9.625	-4	488.04	-32.085	-32.567	-32.326
79	9.625	6	501.95	-20.022	-19.983	-20.002
80	10.313	-9	485.17	-39.771	-40.043	-39.907
81	10.313	1	493.07	-28.452	-27.195	-27.824
82	10.313	11	514.08	-16.989	-16.968	-16.979
83	11	-4	488.46	-36.03	-36.767	-36.398
84	11	6	500.22	-23.933	-23.811	-23.872